EFFECT OF PALLADIUM ON STRUCTURE AND TECHNOLOGICAL PROPERTIES OF Ag–Cu–Zn–Ni–Mn SYSTEM BRAZING FILLER ALLOYS

V.F. KHORUNOV, S.V. MAKSYMOVA and **B.V. STEFANIV**
E.O. Paton Electric Welding Institute, NASU, Kiev, Ukraine

The effect of palladium on structure, melting ranges and technological properties of alloys of the Ag–Cu–Zn–Ni–Mn system was investigated. It was established that alloying with palladium allows improving strength properties of the brazed joints at an insignificant decrease of the contact angle.

Keywords: *brazing, diamond-hard alloy tool, cadmium-free filler alloys, structure, melting range, contact angle, induction heating, phase transformation temperature, palladium, silver filler alloy, strength of joints*

Silver-base cadmium-containing filler alloys are widely applied for brazing of various materials. Considering the negative effect of cadmium on human health, investigations were carried out to determine the possibility of producing cadmium-free filler alloys with the same or similar wetting characteristics and melting temperatures [1–3].

As proved by analysis of literature data, cadmium-free filler alloys of the Ag–Cu–Zn–Ni–Mn system proved well for brazing of diamond-hard alloy tools. Their typical representative is American filler alloy BAg-22. This filler alloy has the following chemical composition, wt.%: 48–50 Ag, 15–17 Cu, 21–25 Zn, 4–5 Ni, 7–8 Mn; T_S = = 680 °C, T_L = 699 °C, and T_{br} = 699–830 °C.

The purpose of this study was to investigate technological properties of a standard filler alloy in brazing of hard alloy plates, determine strength characteristics of the brazed joints and evaluate the possibility of improving the latter due to additional alloying.

Induction heating by using a high-frequency generator of the VChI4-10U4 type with a double-coil inductor was employed to melt experimental alloys of the Ag–Cu–Zn–Ni–Mn and Ag–Cu–Zn–Ni–Mn–Pd systems under laboratory conditions. The filler alloys were melted in alundum crucibles, the latter being placed in graphite crucibles. That is, practically it was radiation heating. First the PV-200 flux was poured into a crucible, then the Ag–Cu–Ni–Mn(Pd) charge placed into a nickel foil was loaded, and after that the flux was poured again. The charge was heated up to its complete melting and formation of the liquid pool. The ingot thus formed was placed into a new crucible, the PV-209 flux was poured, and the alloy was heated up to formation of the liquid pool. Zinc was added in the process of cooling the pool to a temperature of 400–500 °C. This was followed by a short-time heating performed several times to complete melting and achieving the homogeneous melt due to induction and mechanical stirring.

The temperature range of melting of the alloys was determined by differential thermal analysis using the VDTA-8M unit in crucibles made from zirconium oxide. Heating and cooling were performed in the helium atmosphere at a rate of 80 °C/min. Weight of a specimen investigated was 1.25±0.05 g. The specimens were heated twice to provide a good fit of the charge to the crucible bottom and generate reliable data on thermal effects. The thermal effects were fixed from the second heating curve. Solidus and liquidus of the alloy were determined from the heating curve (in cooling of the alloy the substantial effect is exerted by overcooling prior to solidification). At the same time, values of the thermal effects are best seen from the cooling curve of the alloys.

Analysis of the obtained data shows that alloying with palladium exerts a significant effect on the phase transformation temperature and melting range (Table 1; Figure 1, *a*). For instance, only one phase (Figure 1, *b*) was fixed in the Ag–Cu–Zn–Ni–Mn system alloy. The solidus temperature was 670 °C, and the liquidus temperature was 710 °C. In alloy with the 2 % Pd the content the second phase in heating had a non-pronounced thermal effect, but in cooling this effect showed up very clearly (Figure 1, *c*). The solidus temperature was 660 °C and the liquidus temperature was 720 °C, i.e. the solidification range became somewhat wider. Alloy with the 5 % Pd content was also the two-phase one (Figure 1, *d*; Table 2).

Table 1. Melting ranges of commercial filler alloy (1) and alloys under investigation (2–4)

Alloy number	Alloy composition	T_S, °C	T_L, °C
1	40Ag–17Cu–17Zn–26Cd	590	610
2	49Ag–16Cu–23Zn–4.5Ni–7.5Mn	670	710
3	49Ag–16Cu–23Zn–4.5Ni–7.5Mn–2Pd	660	720
4	49Ag–16Cu–23Zn–4.5Ni–7.5Mn–5Pd	670	740

Increase in the palladium concentration led to increase in the solidus and liquidus temperatures (Figure 2).

Metallographic examinations and X-ray spectrum microanalysis of the alloys were conducted on specimens after determination of the melting temperature range. For this all the alloys were cooled down to room temperature at the same cooling rate.

Alloy of the Ag–Cu–Zn–Ni–Mn system had three clearly defined phases (Figure 3, *a*). All of them solidified in close temperature ranges. That is why they had no effect on the thermal curve. It is significant that the solid solution-based primary dendrites contained approximately equal amounts of copper, nickel and zinc, approximately 15 % Mn, but a low amount of silver (Table 2). The silver-based (74.4 %) solid solution solidified in a close temperature range. This phase contained no nickel, the contents of copper and manganese was several times lower, and that of zinc was twice as low. These two phases participated in the process of solidification of the eutectic, the typical structure of which could be seen in some regions (Table 2; Figure 3, *a*).

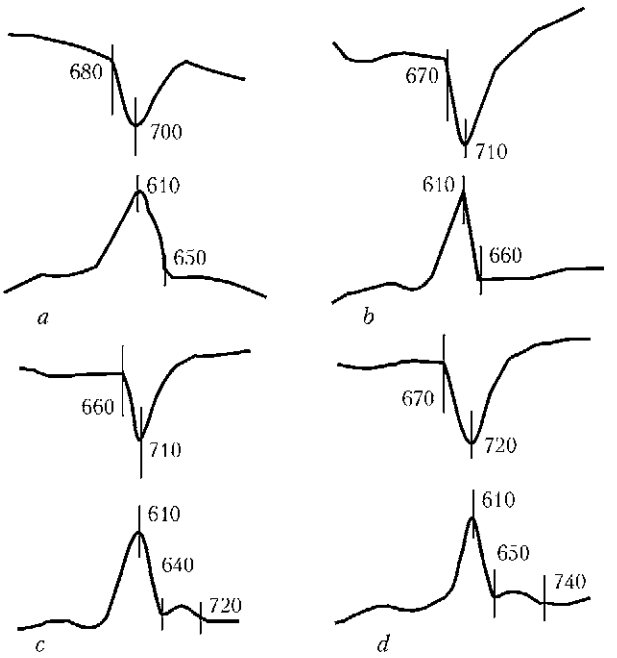

Figure 1. Data of differential thermal analysis of the alloys: *a* — Ag–Cu–Zn–Ni–Mn (amorphous foil); *b* — Ag–Cu–Zn–Ni–Mn (cast); *c* — Ag–Cu–Zn–Mn–2Pd; *d* — Ag–Cu–Zn–Ni–Mn–5Pd

The described solidification mechanism became more pronounced in alloying this composition with palladium. No development of solidification of the primary dendrites (copper-based dark crystals; Figure 3, *b*; Table 2) was detected, as the second phase (silver-based) immediately started solidifying around them. Separate solidification of the phases making up the eutectic took

Table 2. Chemical heterogeneity of the Ag–Cu–Zn–Ni–Mn(Pd) system alloys

Investigated region (phase)	Ag	Cu	Zn	Ni	Mn
49Ag–16Cu–23Zn–4.5Ni–7.5Mn					
Total	49.885	16.894	21.024	6.592	5.607
Dendrite (dark)	4.591	28.938	27.285	24.802	14.987
Grain (light matrix)	74.483	6.692	16.068	0	2.761
Eutectic	58.706	15.784	21.284	1.088	3.139
49Ag–16Cu–23Zn–4.5Ni–7.5Mn–2Pd					
Total	64.541	11.082	16.919	1.044	3.430+(2.995Pd)
Dendrite (dark)	13.696; 11.471	43.421; 34.875	14.573; 25.190	10.905; 14.031	5.274+(12.123Pd)–7.258+(6.162Pd)
Grain (light matrix)	74.810	6.214	16.959	0	2.021+(0Pd)
Eutectic (banded)	67.617; 52.748	9.727; 20.488	15.417; 21.156	1.291; 0.335	2.564–2.219+2.850–3.057Pd
49Ag–16Cu–23Zn–4.5Ni–7.5Mn–5Pd					
Total	63.603	11.371	16.723	1.932	3.239+(3.143Pd)
Dendrite (dark)	8.122	22.072	27.821	13.127	9.753+(19.038Pd)
Grain (light matrix)	70.685	7.437	15.380	0.905	2.676+(2.919Pd)
Eutectic (banded)	60.781; 59.666	13.038; 12.086	17.836; 14.758	1.105; 2.363	2.153+(5.093Pd)–2.963+(8.166Pd)

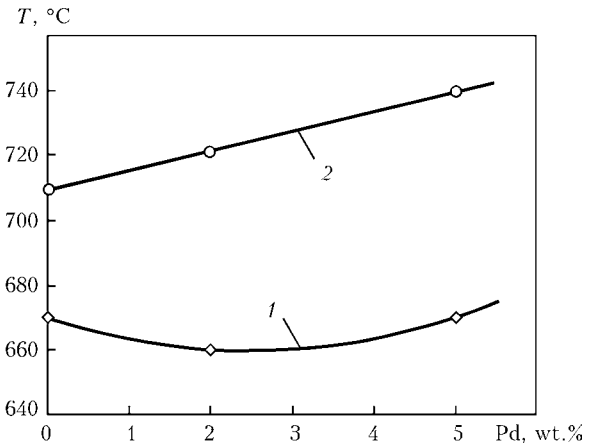

Figure 2. Solidus (*1*) and liquidus (*2*) temperatures of the alloys depending on the palladium content

place first. It was followed by solidification of the normal eutectic occupying the major part of the section. This mechanism was assumed to take place in the study by A.A. Bochvar [4]. However, it is more characteristic of organic materials, and rarely occurs in metal alloys [5]. Note that nickel and palladium were concentrated in dendrites (of a dark colour), and were absent in the light phase (silver-based) (see Figure 3).

Increase in the palladium content of an alloy caused increase in the quantity of the primary crystals. However, they did not grow much, as the silver-based phase started solidifying. The regions of separate solidification of the eutectic occupied the major part of the section. And regions of the normal eutectic occurred much more rarely (Figure 3, *c*). Note that in this alloy the

Table 3. Area of spreading and shear strength of brazed specimens of steel 12Kh18N10T

Filler alloy number	Alloy system	Spreading area S_{spr}, mm^2	Average values of shear strength τ_{sh}, MPa
1	Ag–Cu–Zn–Cd	–	263.3 [6]
2	Ag–Cu–Zn–Ni–Mn	704.7	342.3
3	Ag–Cu–Zn–Ni–Mn–2Pd	573.0	321.3
4	Ag–Cu–Zn–Ni–Mn–5Pd	971.0	359.1

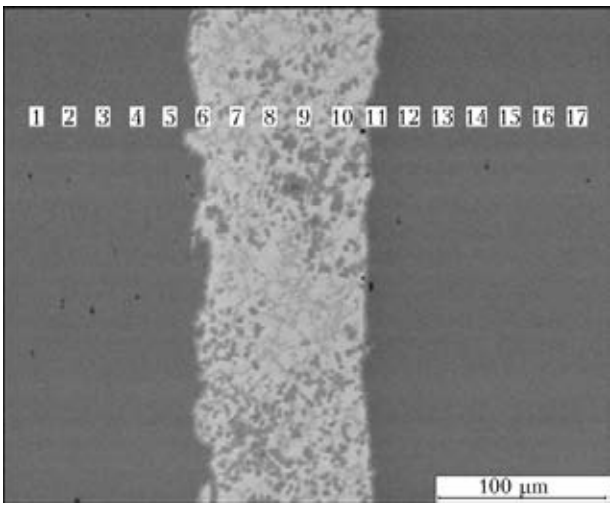

Figure 4. Location of X-ray spectrum analysis points in the brazed seam and base metal

copper-based grains contained a low amount of nickel and palladium.

Experiments on determination of the spreading area over stainless steel and hard-alloy material VK8, as well as strength of the brazed joints produced by joining these materials were carried out by using the investigated brazing filler alloys. The experiments were conducted on stainless steel according to GOST 23904–79 and GOST 23047–75, respectively. The results obtained are given in Table 3.

Structure and chemical heterogeneity of the stainless steel joints produced by using the Ag–Cu–Zn–Ni–Mn system filler alloy were investigated. Structure of the brazed seam turned out to be identical to that of the pure filler alloy: solid solution-based primary dendrites were clearly revealed with the second phase and normal eutectic regions solidifying around them, i.e. there was no intensive development of diffusion exchange at interfaces of the joints. This was proved both by the data of X-ray spectrum microanalysis at separate points (Figure 4; Table 4) and by the diagrams of distribution of elements in cross sections of the seams (Figure 5).

As follows from the data of Table 4, iron and chromium, which are the main elements of the

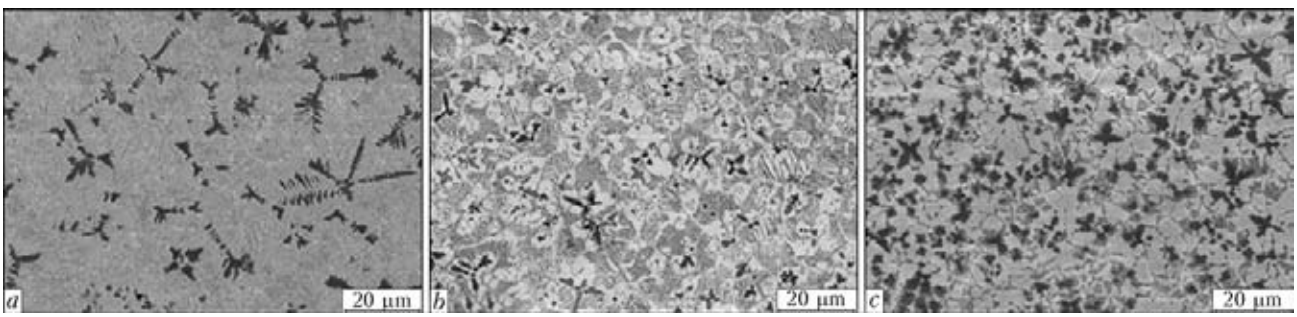

Figure 3. Microstructures of the experimental alloys: *a* — 49Ag–16Cu–23Zn–4.5Ni–7.5Mn; *b* — 49Ag–16Cu–23Zn–4.5Ni–7.5Mn–2Pd; *c* — 49Ag–16Cu–23Zn–4.5Ni–7.5Mn–5Pd

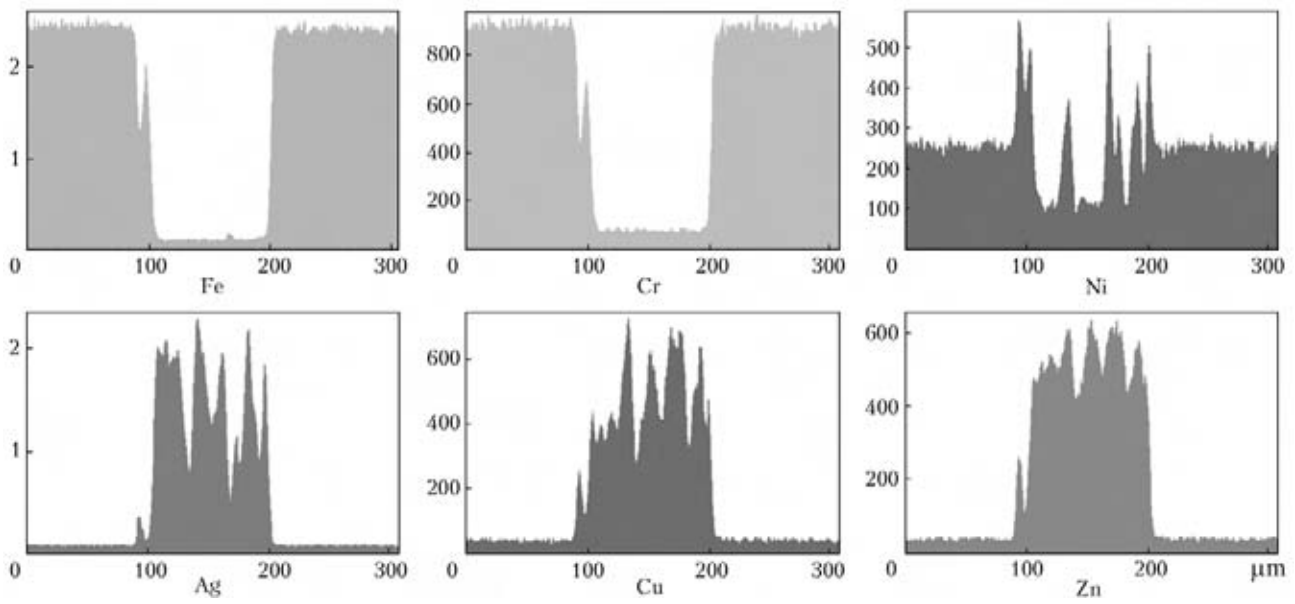

Figure 5. Diagrams of qualitative distribution of elements in the brazed seam metal produced by using the Ag–Cu–Zn–Ni–Mn system filler alloy

brazed metal, were absent in the seam, the transition zone was absent either. The weight content of iron in the base metal near the interface of the joint was 60–70 %, whereas that on the seam side was 0.30–0.75 %. The situation with chromium was similar: near the fusion boundary on the side of the base metal its concentration was 13.5–16.5 %, and on the side of the filler alloy it was 0.18–0.40 %. The seam contained no titanium and silicon at all.

Elements of the filler alloy were present in the seam, and were hardly revealed in the base metal (Table 4). For example, the weight content of silver near the interface of the joint on the seam side was within 65.0–69.5 %, and on the base metal side — within 0–0.97 %. The similar situation was characteristic also of copper and zinc.

The experiments on spreading were carried out by using the 13.5 mm diameter and 4.5 mm

Table 4. Content of elements (wt.%) at separate points of the brazed joint

Spectrum number	Si	Ti	Cr	Mn	Fe	Ni	Cu	Zn	Ag
1	0.6	0.43	17.08	1.8	70.51	9.58	0	0	0
2	0.5	0.38	17.06	1.89	70.62	9.54	0	0	0
3	0.57	0.77	17.6	1.84	69.54	9.68	0	0	0
4	0.7	0.3	16.7	1.33	69.9	11.08	0	0	0
5	0.66	0.52	17.04	2.02	69.45	9.62	0.7	0	0
6	0.26	0.35	13.57	3.4	59.74	17.34	2.51	2.84	0
7	0	0	0.4	0.71	0.3	3.12	13.34	17.13	64.99
8	0	0	0.24	0.67	0.65	2.13	11.33	15.52	69.46
9	0	0	0	0.37	0.23	0.74	8.9	13.4	76.37
10	0.11	0	0	0.95	0.76	4.25	11.59	15.34	67
11	0	0	0.18	0.79	0.75	3.24	11.65	13.79	69.6
12	0.36	0.44	16.56	2.21	70.02	9.43	0	0	0.97
13	0.26	0.71	16.95	2.09	70.91	9.06	0	0	0
14	0.5	0.41	16.99	1.44	70.71	9.95	0	0	0
15	0.6	0.59	17.33	1.71	68.7	9.81	0	0	1.26
16	0.53	0.27	17.18	1.92	70.44	9.67	0	0	0
17	0.34	0.5	17.7	1.62	69.45	9.34	0	0	1.06

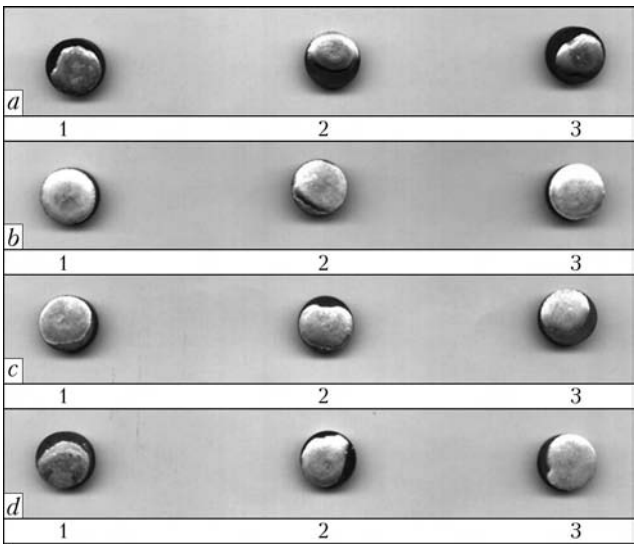

Figure 6. Appearances of specimens 1–3 for investigation of spreading of filler alloys 1–4 (*a–d*) over hard alloy material VK8

thick plates of hard alloy material VK8 and filler alloys in the form of cubes measuring 4 × 4 × × 4 mm.

Prior to brazing the specimens were degreased with acetone (alcohol), then the filler alloy being studied was placed at the specimen centre, and flux of the PV-209 grade having the reactivity temperature range equal to 600–850 °C was deposited on the top over the entire perimeter of a specimen [7]. Heating of the specimens was performed by using high-frequency generator VChI4-10U4 with a frequency of 440 kHz and power of 10 kW. The double-coil inductor was employed for these studies. A rack of heat-resistant ceramics with a channel to attach a thermocouple for measuring the temperature of heating of a specimen up to complete spreading of the filler alloy was installed inside the inductor. Holding for three seconds was performed after melting of the filler alloy. After that heating was stopped. The degree of wetting of a solid substrate with the filler alloys was determined by evaluating the area of spreading of a molten filler alloy (three specimens for each filler alloy) and contact angle between the substrate and a spread droplet of the filler alloy metal (Figure 6). The contact angle was determined on the sections cut out from the specimens normal to the wetting plane (Figure 7). The data were obtained by using the AutoCad software.

Table 5. Results of tests of the VK8 joints brazed with filler alloys of different systems

Filler alloy number	Filler alloy system	Spreading area S_{spr},* mm^2	Contact angle θ, deg	Shear strength τ_{sh}, MPa
1	Ag–Cu–Zn–Cd	95.30	17	245
2	Ag–Cu–Zn–Ni–Mn	136.32	10	225
3	Ag–Cu–Zn–Ni–Mn–2Pd	111.06	16	250
4	Ag–Cu–Zn–Ni–Mn–5Pd	112.01	13	315

*Spreading area was determined by using high-frequency heating following a non-standard procedure

Specimens for mechanical tests were brazed in air by using high-frequency heating. Flux in the form of a paste mixed up with water was preliminarily deposited on the hard alloy plates (VK8+VK8, VK15+VK15 etc.). Then a filler alloy charge was placed between the hard alloy plates, and heating was performed up to complete melting of the flux and filler alloy, as well as up to formation of the joint.

Shear strength was determined by the V.N. Bakul Institute for Superhard Materials of the NAS of Ukraine by using a special attachment (to the tensile testing machine P-05). As seen

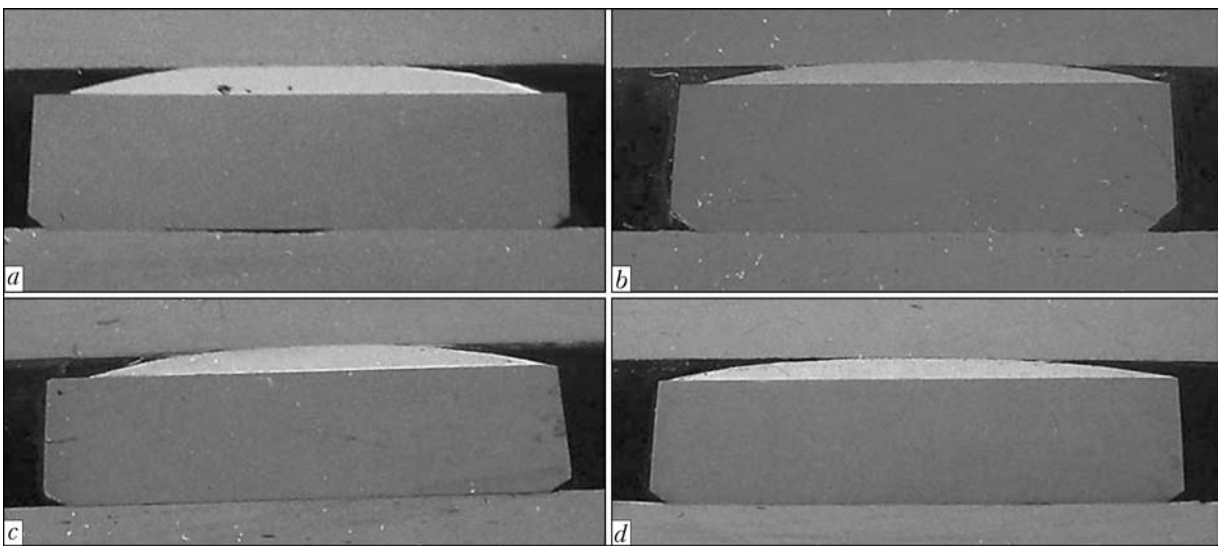

Figure 7. Cross section of specimens after spreading tests using filler alloys 1–4 (*a–d*) (see Table 5)

from the data given in Table 5, alloying of the experimental filler alloy with palladium substantially increased strength of the joints.

Filler alloys of the investigated systems were employed to manufacture a batch of bits for drilling the wells to produce dispersed methane, which increased several times the length of deepening of the wells [8].

Therefore, application of the environmentally clean filler alloys of the Ag–Cu–Zn–Ni–Mn and Ag–Cu–Zn–Ni–Mn–Pd systems instead of filler alloys of the Ag–Cu–Zn–Cd system for brazing of rock and metal cutting tools makes it possible not only to avoid the harmful effect of cadmium on human organism, but also to provide the increased-strength brazed joints.

1. Roberts, P.M. (1978) Recent developments in cadmium-free silver brazing alloys. *Welding J.*, **10**, 23–30.
2. Timmins, P.F. (1994) The development of Ag-based brazing alloys. *Ibid.*, **10**, 31–33.
3. Khorunov, V.F., Maksymova, S.V., Stefaniv, B.V. (2010) Effect of tin additions on structure and technological properties of brazing filler metals of the Ag–Cu–Zn system. *The Paton Welding J.*, **7**, 16–21.
4. Bochvar, A.A. (1956) *Metals science*. Moscow: Metallurgizdat.
5. Taran, Yu.N., Mazur, V.I. (1978) *Structure of eutectic alloys*. Moscow: Metallurgiya.
6. Petrunin, I.E., Lotsmanov, S.N., Nikolaev, G.F. (1973) *Brazing of metals*. Moscow: Metallurgiya.
7. Klochko, N.A. (1981) *Fundamentals of the technology for brazing and heat treatment of hardalloy tool*. Moscow: Metallurgiya.
8. Khorunov, V.F., Maksymova, S.V., Stefaniv, B.V. (2010) Manufacture of drill bits for production of dispersed methane in mine working. *The Paton Welding J.*, **6**, 41–43.

RESEARCH AND DEVELOPMENT OF THE TECHNOLOGY FOR WELDING OF DISSIMILAR HEAT-RESISTANT CHROMIUM AND HIGH-TEMPERATURE STEELS FOR MODERN POWER PLANTS

The research work on the above subject was completed in 2011 by the E.O. Paton Electric Welding Institute (supervisor – Dr. A.K. Tsaryuk)

The object of the research was heat-resistant and high-temperature steels with improved service properties, as well as their welded joints.

The purpose of the research was to identify physical-metallurgical factors that determine formation of structure and mechanical properties of the joints between heat-resistant chromium martensitic steels and high-temperature austenitic steels, and develop the technology for welding these steels.

The research methods included spectral analysis, X-ray spectral microanalysis, metallographic analysis, measurement of hardness and microhardness, and testing of mechanical properties according to GOST 6996–66.

The research showed that welding of martensitic chromium steel of the 10Kh9NMFB type to chrome-nickel steel of the 18-10 type by using austenitic consumables results in structural and chemical heterogeneities taking place in the fusion zone and showing up in formation of soft decarbonised interlayers of structurally free ferrite in HAZ of steel 10Kh9NMFB. Size of this zone decreases with decrease in welding heat input. However, it is impossible to fully avoid it even in welding at minimal heat inputs.

Formation of the ferrite interlayer in HAZ of steel 10Kh9NMFB can be prevented owing to deposition of a purely nickel metal. However, in this case it is impossible to ensure the required service properties of the welded joints. It was established that the ferrite interlayer will not form if steel 10Kh9NMFB is preliminarily coated with martensitic deposited metal.

Lately, along with the traditional technology for welding of dissimilar joints using austenitic-grade consumables, an increasingly wider acceptance is gained by a process that provides for the use of low-carbon chromium filler metal alloyed with nickel, molybdenum, etc.

To ensure strength of the fusion zone at a level of that of steel 08Kh18N10T, it is recommended to preliminarily coat the base metal with materials that provide deposited metal of the 05Kh6M type, while the main volume of the weld can be filled up with both martensitic and austenitic materials.

A new slag system of the fluoride-magnesium type was developed. It provides decrease in the content of carbon in the deposited metal to 0.04 % at a sufficiently low content of diffusible hydrogen. Electrodes developed on the base of this system have good welding-technological properties and provide the deposited metal with optimal chemical composition and mechanical characteristics.